Applied Mathematics and Computation 510 (2026) 129693

Contents lists available at ScienceDirect

Applied Mathematics and Computation

journal homepage: www.elsevier.com/locate/amc

Full Length Article

Secure observer-driven synchronization for complex networks constrained by partial information exchange and limited communication bandwidth

Yan Li [a], Qirun Hang [a], Lijuan Zha [b], Jinliang Liu [c,*]

[a] *College of Computer Science and Artificial Intelligence, Nanjing University of Finance and Economics, Nanjing, Jiangsu, 210023, China*
[b] *College of Science, Nanjing Forestry University, Nanjing, Jiangsu, 210037, China*
[c] *School of Computer Science, Nanjing University of Information Science and Technology, Nanjing, Jiangsu, 210044, China*

ARTICLE INFO

Keywords:
Complex networks (CNs)
Partial information exchange
Synchronization control
False-data-injection (FDI) attack
Weighted try-once-discard (WTOD) protocol

ABSTRACT

This paper addresses the observer-driven secure synchronization control issue for partial information-based complex networks (CNs) subject to bandwidth constraints. Firstly, given that the complete data transmission between CN nodes can not be always realized in practice, the system model of CNs with partial information exchange is specifically introduced. Then, considering the limitation of communication bandwidth, weighted try-once-discard (WTOD) protocol is utilized to enhance the signal transmission efficiency within each node. The delivery of the data adhered to WTOD protocol is further assumed to be compromised by false-data-injection (FDI) attack, which is a well-recognized risk in communication networks. Afterward, distributed secure observer-based synchronization controllers are designed accordingly. Based on defining the observation and synchronization errors, an augmented system model is then established, and the gain matrices for observers and controllers are obtained through an analysis of the stability conditions of the augmented system. Lastly, a numerical example is provided to validate the proposed method's effectiveness.

1. Introduction

Over the past few decades, complex networks (CNs) have been extensively applied to represent various real-world intricate systems, e.g., oral microbial ecosystem [1], climate system [2], and street networks [3]. Typically, a CN is made up of multiple interconnected nodes, each representing an individual entity with distinct dynamic properties [4]. The interconnection among nodes means that there exists information exchange between CN nodes. Actually, the data generated by each node is usually multidimensional, and each dimension may be transmitted via different communication channels [5,6]. Due to the physical constraints and extraneous factors, it is hardly to assure that the information carried on all channels can be delivered successfully, which has been witnessed in many practical scenarios, such as the partial success of excitatory synapse conveying between cortical regions in brain networks [7] and the incomplete data transmission between node pairs in wireless sensor networks [8]. Therefore, it is very significative to investigate CNs with partial information exchange.

Synchronization, as an important dynamic behavior of CNs, will be the first to be affected by partial information transmission given that the data exchange between neighbors is essential for achieving synchronization [9]. In the existed researches, lots of

* Corresponding author.
E-mail addresses: ylnjue@163.com (Y. Li), hangqirun@163.com (Q. Hang), zhalijuan@vip.163.com (L. Zha), liujinliang@vip.163.com (J. Liu).

https://doi.org/10.1016/j.amc.2025.129693
Received 27 February 2025; Received in revised form 10 July 2025; Accepted 15 August 2025
Available online 24 August 2025

synchronization control methods for CNs has been proposed [10–12]. However, the works suppose that the information exchange between coupled nodes can be realized perfectly without any data loss. Taking the partial information exchange into account, Huang et al. [13] introduced a synchronization method for CNs where the imperfect transmission is depicted through diagonal and lower triangular coupling matrices; fixed-time synchronization issue over T-S fuzzy CNs with stochastic effects was investigated in [14]; the prescribed-time synchronization challenge for CNs with specific constraints was examined in [15]. It is further noted that the mentioned efforts for achieving synchronization of CNs with partial information exchange are based on that the system states can be precisely acquired which is hard to be realized in practical systems [16]. In view of this, appropriate observers are widely constructed to efficiently estimate system states and then assist the synchronization of CNs [17–19]. But the observer-based synchronization problem for CNs with partial information exchange has been rarely studied, which primarily motivates our study.

In addition to the challenge incurred by incomplete information transmission, the synchronization of CNs is also impeded by stochastic cyber attacks. In the literature, the commonly concerned attacks include deception attack [20], denial-of-service (DoS) attack [21], replay attack [22] and false-data-injection (FDI) attack [23–25]. Among which, FDI attack poses long-term risk on data integrity given its stealthiness, and then attracts particular consideration. As an illustration, an adaptive event-triggered control method was presented in [26] to achieve synchronization for CNs constrained by FDI attack; Li et al. [27] proposed a periodical secure control strategy for finite-time cluster synchronization of CNs under FDI attack. Therefore, the paper further takes the influence of FDI attack into consideration while studying partial information-based synchronization issue for observer-assisted CNs.

Beyond the destructive malicious impact of FDI attack, the non-malicious effect stemming from the limited communication bandwidth should also be taken seriously [28]. The restriction can lead to data conflict and then result in data loss, which will significantly inhibit the synchronization of CNs. In response to this issue, communication protocols, such as round-robin (RR) protocol [29,30], stochastic communication (SC) protocol [31,32] and weighted try-once-discard (WTOD) protocol [33–35], are extensively employed to schedule the data transmission and thereby preventing data congestion. Among the mentioned protocols, WTOD protocol presents more efficiency and adaptability in delivering critical information. Following WTOD protocol, dynamic weights are allocated to scheduling candidates according to their real-time significance, the candidate with the highest weight will be authorized for data transmission at each moment. Given the merits of WTOD protocol, the exploration of applying it into bandwidth-limited CNs to achieve the desired system performance has been conducted. For instance, Wang et al. [36] developed an $H\infty$ filter for CNs under state saturation and WTOD protocol; Liu et al. [37] investigated set-membership filtering for CNs that using WTOD protocol to enhance data transmission efficiency; a sliding mode control problem over CNs with WTOD protocol and multi-strategy attacks was addressed in [38]. However, there is limited research on the WTOD protocol-based synchronization issue for CNs with finite bandwidth.

Inspired by the above discussion, this paper focuses on partial information-based CNs challenged by FDI attack and limited bandwidth, and then devotes to propose WTOD protocol-enabled control method to obtain the synchronization of the CNs. The contributions of the study can be summarized as follows.

1) WTOD protocol is employed to arrange the data transmission within each subsystem of partial information-based CNs so as to assist the synchronization of the CNs under bandwidth-constrained communication scenario.
2) The stochastic characteristic and destruction on data integrity of FDI attack are effectively depicted, and then distributed observer-based secure synchronization controllers are constructed for the CNs with WTOD protocol and partial information exchange.
3) The parameters of the designed observers and controllers are derived based on establishing an augmented synchronization error system and analyzing the sufficient conditions for the asymptotic stability of the system.

The rest of the paper is organized as follows. Section 2 gives the specific problem description of the studied observer-based synchronization issue for a CN affected by partial information exchange, potential data collision and FDI attack. In Section 3, the sufficient conditions for achieving the desired synchronization of the considered CN are derived, and then the approach for calculating the designed observers and controllers' gains is proposed. Section 4 assesses the performance of the proposed synchronization control strategy via conducting simulations. The conclusion of the paper is finally presented in Section 5.

2. Problem description

In this section, the model of the CN with partial information exchange is firstly introduced, which is followed by the mathematical depiction of the impacts of WTOD protocol and FDI attack. Based on these, the framework of the observer-based controllers is presented, and then the problem formulation is given by establishing an augmented synchronization error system.

2.1. System model

We consider a discrete-time CN with N nodes, and the architecture of each node is presented by Fig. 1. The system model of node i $(1 \le i \le N)$ is described as below:

$$\begin{cases} x_i(\varsigma+1) = Ax_i(\varsigma) + g(x_i(\varsigma)) + \rho \sum_{j=1}^{N} w_{ij} H_{ij} \Gamma x_j(\varsigma) + Bu_i(\varsigma), \\ y_i(\varsigma) = Cx_i(\varsigma), \end{cases} \tag{1}$$

where $x_i(\varsigma) \in \mathbb{R}^n$, $y_i(\varsigma) \in \mathbb{R}^p$ and $u_i(\varsigma) \in \mathbb{R}^q$ are the system state, measurement output and control input of node i, respectively; $g(.)$ is a nonlinear function; $w_{ij} > 0$ $(1 \le j \ne i \le N)$ denotes the outer coupling relationship between node i and node j, where it

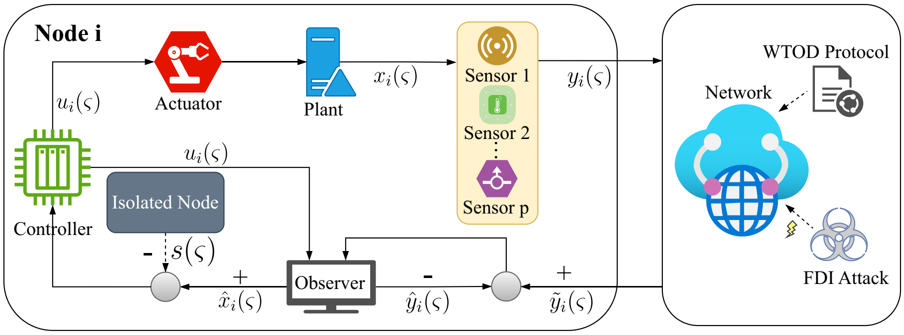

Fig. 1. System architecture of each node in the considered CN.

is assumed that $w_{ii} = -\sum_{j=1,j\neq i}^{N} w_{ij}$; $\Gamma = diag\{\gamma_1, \gamma_2, \ldots, \gamma_n\}$ is the inner coupling matrix, and $\rho > 0$ is the system coupling strength; $H_{ij} = diag\{h_{ij}^1, h_{ij}^2, \ldots, h_{ij}^n\}$ is the channel matrix, in which each binary variable h_{ij}^{ω} $(1 \le \omega \le n)$ indicates whether the ω-th channel from node j to node i is active; A, B and C are system parameter matrices with suitable dimensions.

Remark 1. In the system model (1), the matrix H_{ij} well depicts the influence of partial information exchange. Specifically, given that $x_j(\varsigma) = [x_{j1}(\varsigma), x_{j2}(\varsigma), \cdots, x_{jn}(\varsigma)]^T$, it has $h_{ij}^{\omega} x_{j\omega}(\varsigma) = x_{j\omega}(\varsigma)$ if $h_{ij}^{\omega} = 1$, which implies that the w-th dimension of $x_j(\varsigma)$ can be successfully received by node i, otherwise $h_{ij}^{\omega} x_{j\omega}(\varsigma) = 0$ which denotes the loss of $x_{j\omega}(\varsigma)$ for node i. Then, $H_{ij}x_j(\varsigma) = [h_{ij}^1 x_{j1}(\varsigma), h_{ij}^2 x_{j2}(\varsigma), \cdots, h_{ij}^n x_{jn}(\varsigma)]^T$ describes the information received by node i from node j under the scenario of partial information exchange.

Assumption 1. [26] The nonlinear function $g(.)$ satisfies the following Lipschitz constraint:

$$||g(a) - g(b)|| \le ||U(a - b)||, \tag{2}$$

where U is a constant matrix representing the upper bound of $g(\cdot)$.

The introduced CN is further assumed to be constrained by limited communication bandwidth and FDI attack, thus we then illustrate how to use WTOD protocol to arrange the data transmission so as to avoid data collision incurred by the bandwidth limitation and depict the influence of the considered attack.

2.2. WTOD Protocol and FDI attack

Without loss of generality, the following illustration will focus on node i. To simplify the description, we firstly let $R_{ij} = w_{ij}H_{ij}$ for $1 \le i \ne j \le N$ and $R_{ii} = -\sum_{j=1,j\neq i}^{N} R_{ij}$, then rewrite (1) as below:

$$\begin{cases} x_i(\varsigma+1) = Ax_i(\varsigma) + g(x_i(\varsigma)) + \rho\sum_{j=1}^{N} R_{ij}\Gamma x_j(\varsigma) + Bu_i(\varsigma), \\ y_i(\varsigma) = Cx_i(\varsigma). \end{cases} \tag{3}$$

For the measurement output $y_i(\varsigma)$, which is supposed to be acquired by p sensors as shown in Fig. 1, the information of p dimensions, i.e., $y_{i\varpi}(\varsigma)$ $(1 \le \varpi \le p)$, will be scheduled by WTOD protocol for realizing conflict-free data transmission under limited communication bandwidth. By employing WTOD protocol, the dimension with the largest fluctuation will be released into the network, to be specific, let $f_i(\varsigma)$ be the index of the sensor that is selected to transmit its generated signal at time instant ς, then it has:

$$f_i(\varsigma) = \arg\max_{1\le\varpi\le p} (y_{i\varpi}(\varsigma) - \check{y}_{i\varpi}(\varsigma))^T Q_{i\varpi}(y_{i\varpi}(\varsigma) - \check{y}_{i\varpi}(\varsigma)), \tag{4}$$

where $\check{y}_{i\varpi}(\varsigma)$ denotes the most recent transmitted signal from sensor ϖ before time instant ς, $Q_{i\varpi}$ represents a positive-definite weight matrix designated for sensor ϖ, and it is obviously that $f_i(\varsigma) \in \{1, 2, \cdots, p\}$. As described by Eq. (4), at each time instant ς, the weighted norm of the difference between the current measurement $y_{i\varpi}(\varsigma)$ and the most recently transmitted signal $\check{y}_{i\varpi}(\varsigma)$ for each sensor ϖ is evaluated by introducing $Q_{i\varpi}$, then the one with the largest weighted deviation is prioritized for transmission, where $Q_{i\varpi}$ enables flexible sensitivity tuning for each sensor to reflect its relative importance.

Based on the function of WTOD protocol, we further update $y_{i\varpi}(\varsigma)$ as follows:

$$\bar{y}_{i\varpi}(\varsigma) = \begin{cases} y_{i\varpi}(\varsigma), & if \quad \varpi = f_i(\varsigma), \\ 0, & otherwise. \end{cases} \tag{5}$$

To facilitate the subsequent analysis, we then introduce the Kronecker delta function $\delta(\cdot) \in \{0, 1\}$, and define $\Pi_{f_i(\varsigma)} = \mathrm{diag}\{\delta(f_i(\varsigma) - 1), \delta(f_i(\varsigma) - 2), \ldots, \delta(f_i(\varsigma) - p)\}$, then the overall measured output, i.e., $\bar{y}_i(\varsigma) = [\bar{y}_{i1}(\varsigma), \bar{y}_{i2}(\varsigma), \ldots, \bar{y}_{ip}(\varsigma)]^T$, can be inferred as:

$$\bar{y}_i(\varsigma) = \Pi_{f_i(\varsigma)} y_i(\varsigma). \tag{6}$$

Actually, the measured signal selected based on WTOD protocol, i.e., $y_{if_i(\varsigma)}(\varsigma)$, may not be securely delivered over the network due to the occurrence of FDI attack. Given the stochastic nature of cyber attacks [39], a Bernoulli variable $\alpha_i(\varsigma) \in \{0, 1\}$ with $\mathrm{Prob}\{\alpha_i(\varsigma) =$

$1\} = \bar{\alpha}_i$ and $\text{Prob}\{\alpha_i(\varsigma) = 0\} = 1 - \bar{\alpha}_i$, where $0 \le \bar{\alpha}_i \le 1$, is introduced to describe whether the attack is successfully launched at each time instant; moreover, an energy-bounded function $\hbar_i(\varsigma) \in \mathbb{R}^p$ is used to portray the specific influence of the attack on the transmitted signal. Then, the attack-affected overall measured output, denoted as $\tilde{y}_i(\varsigma)$, is defined as:

$$\tilde{y}_i(\varsigma) = \bar{y}_i(\varsigma) + \alpha_i(\varsigma)\Pi_{f_i(\varsigma)}\hbar_i(\varsigma). \tag{7}$$

Assumption 2. [34] For the attack function $\hbar_i(\varsigma)$, it is supposed to be bounded by the following constraint:

$$\hbar_i^T(\varsigma)\hbar_i(\varsigma) \le x_i^T(\varsigma)F^T F x_i(\varsigma), \tag{8}$$

where F is a known constant matrix representing the upper bound of $\hbar_i(\varsigma)$.

Remark 2. As reflected in Eqs. (7) and (8), energy-bounded malicious data will be injected into measurement output if the FDI attack is successfully launched. Given that the real-time data can still be received by the observer and the amplitude of attack signal is bounded, it is challenging to implement a timely attack defense, which highlights the importance of design secure synchronization control method for the considered CN.

2.3. Design of observer and controller

For the above described CN, we then dedicate to design observer-based synchronization controller for each node i. For this, an isolated node with the following dynamics is firstly introduced.

$$s(\varsigma + 1) = As(\varsigma) + g(s(\varsigma)), \tag{9}$$

where $s(\varsigma) \in \mathbb{R}^n$ denotes the state of the isolated node. Then, the devised observer is presented as below:

$$\begin{cases} \hat{x}_i(\varsigma + 1) = A\hat{x}_i(\varsigma) + g(\hat{x}_i(\varsigma)) + \rho \sum_{j=1}^N R_{ij}\Gamma\hat{x}_j(\varsigma) + Bu_i(\varsigma) + L_{i,f_i(\varsigma)}(\tilde{y}_i(\varsigma) - \hat{y}_i(\varsigma)), \\ \hat{y}_i(\varsigma) = C\hat{x}_i(\varsigma), \end{cases} \tag{10}$$

where $\hat{x}_i(\varsigma)$ and $\hat{y}_i(\varsigma)$ represent the estimations of $x_i(\varsigma)$ and $y_i(\varsigma)$, respectively; $L_{i,f_i(\varsigma)} \in \mathbb{R}^{n\times p}$ are the observer gains which will be determined shortly. The isolated node is co-located with node i as shown in Fig. 1, thus based on the description of the isolated node and observer, the synchronization controller is designed as:

$$u_i(\varsigma) = K_{i,f_i(\varsigma)}(\hat{x}_i(\varsigma) - s(\varsigma)), \tag{11}$$

where $K_{i,f_i(\varsigma)} \in \mathbb{R}^{n\times n}$ indicate the controller gains which need to be properly determined.

2.4. Problem formulation

Let $\hat{e}_i(\varsigma) = x_i(\varsigma) - \hat{x}_i(\varsigma)$ and $e_i(\varsigma) = x_i(\varsigma) - s(\varsigma)$ be the estimation error and synchronization error, respectively, then based on Eqs. (3) and (10), it can be obtained that:

$$\begin{aligned} \hat{e}_i(\varsigma + 1) &= x_i(\varsigma + 1) - \hat{x}_i(\varsigma + 1) = A\hat{e}_i(\varsigma) + g(\hat{e}_i(\varsigma)) + \rho \sum_{j=1}^N R_{ij}\Gamma\hat{e}_j(\varsigma) - L_{i,f_i(\varsigma)}(\tilde{y}_i(\varsigma) - \hat{y}_i(\varsigma)) \\ &= A\hat{e}_i(\varsigma) + g(\hat{e}_i(\varsigma)) + \rho \sum_{j=1}^N R_{ij}\Gamma\hat{e}_j(\varsigma) - L_{i,f_i(\varsigma)}(\Pi_{f_i(\varsigma)}Cx_i(\varsigma) + \alpha_i(\varsigma)\Pi_{f_i(\varsigma)}\hbar_i(\varsigma) - C\hat{x}_i(\varsigma)), \end{aligned} \tag{12}$$

where $g(\hat{e}_i(\varsigma)) = g(x_i(\varsigma)) - g(\hat{x}_i(\varsigma))$; furthermore, according to Eqs. (3) and (9), it has:

$$e_i(\varsigma + 1) = x_i(\varsigma + 1) - s(\varsigma + 1) = Ae_i(\varsigma) + g(e_i(\varsigma)) + \rho \sum_{j=1}^N R_{ij}\Gamma e_j(\varsigma) + BK_{i,f_i(\varsigma)}(\hat{x}_i(\varsigma) - s(\varsigma)), \tag{13}$$

where $g(e_i(\varsigma)) = g(x_i(\varsigma)) - g(s(\varsigma))$.

By integrating the information of N nodes, the overall system state, estimation and synchronization errors can be expressed as follows:

$$x(\varsigma + 1) = \bar{A}x(\varsigma) + G_x(\varsigma) + \rho\bar{\Gamma}x(\varsigma) + \bar{B}K_{f(\varsigma)}(e(\varsigma) - \hat{e}(\varsigma)) = (\bar{A} + \rho\bar{\Gamma})x(\varsigma) + G_x(\varsigma) + \bar{B}K_{f(\varsigma)}e(\varsigma) - \bar{B}K_{f(\varsigma)}\hat{e}(\varsigma), \tag{14}$$

$$\begin{aligned} e(k + 1) &= \bar{A}e(\varsigma) + G(\varsigma) + \rho\bar{\Gamma}e(\varsigma) + \bar{B}K_{f(\varsigma)}(e(\varsigma) - \hat{e}(\varsigma)) = (\bar{A} + \rho\bar{\Gamma})e(\varsigma) + G(\varsigma) + +\bar{B}K_{f(\varsigma)}e(\varsigma) - \bar{B}K_{f(\varsigma)}\hat{e}(\varsigma) \\ &= (\bar{A} + \rho\bar{\Gamma} + \bar{B}K_{f(\varsigma)})e(\varsigma) + G(\varsigma) - \bar{B}K_{f(\varsigma)}\hat{e}(\varsigma), \end{aligned} \tag{15}$$

$$\begin{aligned} \hat{e}(k + 1) &= \bar{A}\hat{e}(\varsigma) + \hat{G}(\varsigma) + \rho\bar{\Gamma}\hat{e}(\varsigma) - L_{f(\varsigma)}(\bar{\Pi}_{f(\varsigma)}\bar{C}x(\varsigma) + \alpha(\varsigma)\bar{\Pi}_{f(\varsigma)}\hbar(\varsigma) - \bar{C}\hat{x}(\varsigma)) \\ &= (\bar{A} + \rho\bar{\Gamma})\hat{e}(\varsigma) + \hat{G}(\varsigma) - L_{f(\varsigma)}\bar{\Pi}_{f(\varsigma)}\bar{C}x(\varsigma) - \alpha(\varsigma)L_{f(\varsigma)}\bar{\Pi}_{f(\varsigma)}\hbar(\varsigma) + L_{f(\varsigma)}\bar{C}(x(\varsigma) - \hat{e}(\varsigma)) \\ &= (L_{f(\varsigma)}\bar{C} - L_{f(\varsigma)}\bar{\Pi}_{f(\varsigma)}\bar{C})x(\varsigma) + (\bar{A} + \rho\bar{\Gamma} - L_{f(\varsigma)}\bar{C})\hat{e}(\varsigma) + \hat{G}(\varsigma) - \alpha(\varsigma)L_{f(\varsigma)}\bar{\Pi}_{f(\varsigma)}\hbar(\varsigma), \end{aligned} \tag{16}$$

where

$$\bar{\Gamma} = \begin{bmatrix} R_{11}\Gamma & R_{12}\Gamma & \cdots & R_{1N}\Gamma \\ R_{21}\Gamma & R_{22}\Gamma & \cdots & R_{2N}\Gamma \\ \vdots & \vdots & \ddots & \vdots \\ R_{N1}\Gamma & R_{N2}\Gamma & \cdots & R_{NN}\Gamma \end{bmatrix},$$

$$
\begin{aligned}
&x(\varsigma) = \mathrm{col}_N\{x_i(\varsigma)\}, && \hat{x}(\varsigma) = \mathrm{col}_N\{\hat{x}_i(\varsigma)\}, && e(\varsigma) = \mathrm{col}_N\{e_i(\varsigma)\},\\
&\hat{e}(\varsigma) = \mathrm{col}_N\{\hat{e}_i(\varsigma)\}, && G(\varsigma) = \mathrm{col}_N\{g(e_i(\varsigma))\}, && G_x(\varsigma) = \mathrm{col}_N\{g(x_i(\varsigma))\},\\
&\hat{G}(\varsigma) = \mathrm{col}_N\{g(\hat{e}_i(\varsigma))\}, && \bar{A} = \mathrm{diag}_N\{A\}, && \bar{B} = \mathrm{diag}_N\{B\},\\
&\bar{C} = \mathrm{diag}_N\{C\}, && L_{f(\varsigma)} = \mathrm{diag}_N\{L_{i,f_i(\varsigma)}\}, && K_{f(\varsigma)} = \mathrm{diag}_N\{K_{i,f_i(\varsigma)}\},\\
&\bar{\Pi}_{f(\varsigma)} = \mathrm{diag}_N\{\Pi_{f_i(\varsigma)}\}, && \hbar(\varsigma) = \mathrm{col}_N\{\hbar_i(\varsigma)\}, && \alpha(\varsigma) = \mathrm{diag}_N\{\alpha_i(\varsigma)\},\\
&f(\varsigma) \in \{1, 2, \cdots, \varepsilon\}, && \varepsilon = p^N.
\end{aligned}
$$

Based on Eqs. (14)–(16) and defining $\xi(\varsigma) = [x^T(\varsigma)\ \ e^T(\varsigma)\ \ \hat{e}^T(\varsigma)]^T$, the following augmented system can then be derived.

$$\xi(\varsigma+1) = \Omega_{f(\varsigma)}\xi(\varsigma) + \omega(\varsigma) + \bar{\alpha}(\varsigma)D_{f(\varsigma)}\bar{\hbar}(\varsigma), \tag{17}$$

where

$$
\begin{aligned}
&\Omega_{f(\varsigma)} = \begin{bmatrix} \bar{A}+\rho\bar{\Gamma} & \bar{B}K_{f(\varsigma)} & -\bar{B}K_{f(\varsigma)} \\ 0 & \bar{A}+\rho\bar{\Gamma}+\bar{B}K_{f(\varsigma)} & -\bar{B}K_{f(\varsigma)} \\ L_{f(\varsigma)}\bar{C} - L_{f(\varsigma)}\bar{\Pi}_{f(\varsigma)}\bar{C} & 0 & \bar{A}+\rho\bar{\Gamma}-L_{f(\varsigma)}\bar{C} \end{bmatrix},\\
&\omega(\varsigma) = [G_x^T(\varsigma)\ \ G^T(\varsigma)\ \ \hat{G}^T(\varsigma)]^T, \qquad \bar{\alpha}(\varsigma) = \mathrm{diag}\{\alpha(\varsigma),\ \alpha(\varsigma),\ \alpha(\varsigma)\},\\
&D_{f(\varsigma)} = \mathrm{diag}\{0,\ 0,\ -L_{f(\varsigma)}\bar{\Pi}_{f(\varsigma)}\}, \qquad \bar{\hbar}(\varsigma) = [\hbar^T(\varsigma)\ \ \hbar^T(\varsigma)\ \ \hbar^T(\varsigma)]^T.
\end{aligned}
$$

Then, the study aims to develop an efficient observer-based synchronization control approach to guarantee the stability of the augmented system as indicated by Eq. (17). Apparently, the above augmented model achieves holistic system description, coordinated performance improvement, and simplified stability analysis. Before concluding this section, the following lemma is provided to facilitate the subsequent analysis.

Lemma 1. *[34] For a full-rank matrix $\kappa \in \mathbb{R}^{n\times q}$, the singular value decomposition (SVD) of κ can be expressed as follows:*

$$\kappa = \vartheta\begin{bmatrix} S \\ 0 \end{bmatrix}\nu^T,$$

where ϑ and ν are orthogonal matrices, with $\vartheta^T\vartheta = I$ and $\nu^T\nu = I$. Then, given matrices $\chi > 0$, $M \in \mathbb{R}^{n\times n}$, and $N \in \mathbb{R}^{q\times n}$, the existence of a matrix $\bar{\chi}$ satisfying $\bar{\chi}\kappa = \kappa\chi$ depends on the fulfillment of the following condition:

$$\chi = \vartheta\begin{bmatrix} M & 0 \\ 0 & N \end{bmatrix}\vartheta^T.$$

3. Main results

In this section, we explore the sufficient conditions that ensure the asymptotic stability of the established system described by Eq. (17) in Theorem 1. Then, in Theorem 2, we derive the observers and controllers' gains based on the obtained conditions.

Theorem 1. *Given the positive scalars $\bar{\alpha}_i$ $(1 \le i \le N)$, gain matrices L_z and K_z $(z = 1, 2, \cdots, \varepsilon)$, the asymptotic stability of the constructed system depicted by Eq. (17) can be achieved if there exist positive-definite matrices $P_z > 0$ with suitable dimensions such that the following inequalities can hold.*

$$\begin{bmatrix} \Theta_z & * \\ \nabla_z & -P_l^{-1} \end{bmatrix} < 0, \tag{18}$$

where

$$
\begin{aligned}
&P_z = diag\{P_{z,1},\ P_{z,2},\ P_{z,3}\}, \quad \Theta_z = \begin{bmatrix} -P_z + \bar{U}^T\bar{U} + \tilde{F}^T\tilde{F} & 0 & 0 \\ 0 & -I & 0 \\ 0 & 0 & -I \end{bmatrix},\\
&\tilde{F} = diag\{\bar{F}, 0, 0\}, \quad \bar{F} = diag_N\{\sqrt{3}F\}, \quad \bar{U} = diag\{\tilde{U}, \tilde{U}, \tilde{U}\},\\
&\tilde{U} = diag_N\{U\}, \quad \nabla_z = [\Omega_z\ \ I\ \ \tilde{\alpha}D_z], \quad \bar{\alpha} = diag_N\{\bar{\alpha}_i\},\\
&\breve{\alpha} = diag\{\bar{\alpha},\ \bar{\alpha},\ \bar{\alpha}\}, \quad \tilde{\alpha} = \breve{\alpha} + \sqrt{\breve{\alpha}(I-\breve{\alpha})}.
\end{aligned}
$$

Proof. Constructing the Lyapunov function as follows:

$$V(\varsigma) = \xi^T(\varsigma)P_{f(\varsigma)}\xi(\varsigma). \tag{19}$$

The forward difference of $V(\varsigma)$ is defined as $\Delta V(\varsigma) = V(\varsigma+1) - V(\varsigma)$. Then, we can get:

$$
\begin{aligned}
E\{\Delta V(\varsigma)\} &= E\{V(\varsigma+1) - V(\varsigma)\} = E\{\xi^T(\varsigma+1)P_{f(\varsigma+1)}\xi(\varsigma+1) - \xi^T(\varsigma)P_{f(\varsigma)}\xi(\varsigma)\}\\
&= E\{\xi^T(\varsigma+1)P_{f(\varsigma+1)}\xi(\varsigma+1)\} - E\{\xi^T(\varsigma)P_{f(\varsigma)}\xi(\varsigma)\},
\end{aligned}
\tag{20}
$$

The first item in the above equation can be further expressed as:

$$\begin{aligned}E\{\xi^T(\varsigma+1)P_{f(\varsigma+1)}\xi(\varsigma+1)\} &= E\{[\Omega_{f(\varsigma)}\xi(\varsigma)+\omega(\varsigma)+\bar{\alpha}(\varsigma)D_{f(\varsigma)}\bar{\hbar}(\varsigma)]^T P_{f(\varsigma+1)}\times[\Omega_{f(\varsigma)}\xi(\varsigma)+\omega(\varsigma)+\bar{\alpha}(\varsigma)D_{f(\varsigma)}\bar{\hbar}(\varsigma)]\}\\ &= E\{[\Omega_{f(\varsigma)}\xi(\varsigma)+\omega(\varsigma)+\breve{\alpha}D_{f(\varsigma)}\bar{\hbar}(\varsigma)+(\bar{\alpha}(\varsigma)-\breve{\alpha})D_{f(\varsigma)}\bar{\hbar}(\varsigma)]^T P_{f(\varsigma+1)}\\ &\quad\times[\Omega_{f(\varsigma)}\xi(\varsigma)+\omega(\varsigma)+\breve{\alpha}D_{f(\varsigma)}\bar{\hbar}(\varsigma)+(\bar{\alpha}(\varsigma)-\breve{\alpha})D_{f(\varsigma)}\bar{\hbar}(\varsigma)]\}\\ &= [\Omega_{f(\varsigma)}\xi(\varsigma)+\omega(\varsigma)+\breve{\alpha}D_{f(\varsigma)}\bar{\hbar}(\varsigma)]^T P_{f(\varsigma+1)}[\Omega_{f(\varsigma)}\xi(\varsigma)+\omega(\varsigma)\\ &\quad+\breve{\alpha}D_{f(\varsigma)}\bar{\hbar}(\varsigma)]+\breve{\alpha}(I-\breve{\alpha})[D_{f(\varsigma)}\bar{\hbar}(\varsigma)]^T P_{f(\varsigma+1)}[D_{f(\varsigma)}\bar{\hbar}(\varsigma)].\end{aligned} \tag{21}$$

Based on Assumption 1, we can derive the following inequality:

$$\omega^T(\varsigma)\omega(\varsigma)\le\xi^T(\varsigma)\bar{U}^T\bar{U}\xi(\varsigma). \tag{22}$$

Moreover, according to Assumption 2, it can be obtained that:

$$\bar{\hbar}^T(\varsigma)\bar{\hbar}(\varsigma)\le x^T(\varsigma)\bar{F}^T\bar{F}x(\varsigma). \tag{23}$$

Then, by referring to Eqs. (20)–(23), it has:

$$\begin{aligned}E\{\Delta V(\varsigma)\} &\le [\Omega_{f(\varsigma)}\xi(\varsigma)+\omega(\varsigma)+\breve{\alpha}D_{f(\varsigma)}\bar{\hbar}(\varsigma)]^T P_{f(\varsigma+1)}[\Omega_{f(\varsigma)}\xi(\varsigma)+\omega(\varsigma)+\breve{\alpha}D_{f(\varsigma)}\bar{\hbar}(\varsigma)]+\breve{\alpha}(I-\breve{\alpha})[D_{f(\varsigma)}\bar{\hbar}(\varsigma)]^T P_{f(\varsigma+1)}[D_{f(\varsigma)}\bar{\hbar}(\varsigma)]\\ &\quad-\xi^T(\varsigma)P_{f(\varsigma)}\xi(\varsigma)+\xi^T(\varsigma)\bar{U}^T\bar{U}\xi(\varsigma)-\omega^T(\varsigma)\omega(\varsigma)+x^T(\varsigma)\bar{F}^T\bar{F}x(\varsigma)-\bar{\hbar}^T(\varsigma)\bar{\hbar}(\varsigma)\\ &= [\Omega_{f(\varsigma)}\xi(\varsigma)+\omega(\varsigma)+\breve{\alpha}D_{f(\varsigma)}\bar{\hbar}(\varsigma)]^T P_{f(\varsigma+1)}[\Omega_{f(\varsigma)}\xi(\varsigma)+\omega(\varsigma)+\breve{\alpha}D_{f(\varsigma)}\bar{\hbar}(\varsigma)]+\breve{\alpha}(I-\breve{\alpha})[D_{f(\varsigma)}\bar{\hbar}(\varsigma)]^T P_{f(\varsigma+1)}[D_{f(\varsigma)}\bar{\hbar}(\varsigma)]\\ &\quad+\beta^T(\varsigma)\Theta_{f(\varsigma)}\beta(\varsigma),\end{aligned} \tag{24}$$

where

$$\beta(\varsigma)=[\xi^T(\varsigma),\ \omega^T(\varsigma),\ \bar{\hbar}^T(\varsigma)]^T,$$

$$\Theta_{f(\varsigma)}=\begin{bmatrix}-P_{f(\varsigma)}+\bar{U}^T\bar{U}+\bar{F}^T\bar{F} & 0 & 0\\ 0 & -I & 0\\ 0 & 0 & -I\end{bmatrix}.$$

On the basis of Eq. (24) and employing the Schur complement method, it can be concluded that $E\{\Delta V(\varsigma)\}<0$ is guaranteed with the holding of the conditions specified in Eq. (18), which means the achievement of the asymptotic stability of the system Eq. (17). So far, the proof is completed. □

As shown in Theorem 1, the conditions for assuring the stability of the established system are derived based on the given gain matrices, which means that our objective remains unachieved. Thus, Theorem 2 is then presented to introduce how to calculate the observers and controllers' gains.

Theorem 2. *Given the positive scalars $\bar{\alpha}_i$ $(1\le i\le N)$, the asymptotic stability of the constructed system as defined by Eq. (17), can be guaranteed if a positive-definite matrix $X>0$ and matrices Y_z and Z_z $(z=1,2,\dots,\varepsilon)$ of suitable dimensions exist, ensuring the satisfaction of the following linear matrix inequalities (LMIs).*

$$\begin{bmatrix}\Theta_z & *\\ \bar{\nabla}_z & -\tilde{P}_x\end{bmatrix}<0, \tag{25}$$

where

$$\bar{\nabla}_z=[\bar{\Omega}_z\ \ \bar{X}\ \ \tilde{\alpha}\bar{D}_z],$$

$$\bar{\Omega}_z=\begin{bmatrix}X(\bar{A}+\rho\bar{\Gamma}) & \bar{B}Y_z & -\bar{B}Y_z\\ 0 & X(\bar{A}+\rho\bar{\Gamma})+\bar{B}Y_z & -\bar{B}Y_z\\ Z_z\bar{C}-Z_z\bar{\Pi}_z\bar{C} & 0 & X(\bar{A}+\rho\bar{\Gamma})-Z_z\bar{C}\end{bmatrix},$$

$$\bar{X}=diag\{X,X,X\},\qquad \tilde{D}_z=diag\{0,\ 0,\ -Z_z\bar{\Pi}_z\},$$

$$\tilde{P}_x=diag\{P_{l,1}-X-X^T,\ P_{l,2}-X-X^T,\ P_{l,3}-X-X^T\}.$$

Proof. Firstly, by pre-multiplying and post-multiplying the left side of Eq. (18) with $\mathrm{diag}\{I,I,I,I,I,I,I,X,X,X\}$ and $\mathrm{diag}\{I,I,I,I,I,I,I,X^T,X^T,X^T\}$, respectively, we can obtain that:

$$\begin{bmatrix}\Theta_z & *\\ \tilde{\nabla}_z & -P_x\end{bmatrix}<0, \tag{26}$$

where

$$\tilde{\nabla}_z=[\tilde{\Omega}_z\ \ \bar{X}\ \ \tilde{\alpha}\tilde{D}_z],\qquad \tilde{D}_z=\mathrm{diag}\{0,\ 0,\ -XL_z\bar{\Pi}_z\},$$

$$\tilde{\Omega}_z=\begin{bmatrix}X(\bar{A}+\rho\bar{\Gamma}) & X\bar{B}K_z & -X\bar{B}K_z\\ 0 & X(\bar{A}+\rho\bar{\Gamma}+\bar{B}K_z) & -X\bar{B}K_z\\ X(L_z\bar{C}-L_z\bar{\Pi}_z\bar{C}) & 0 & X(\bar{A}+\rho\bar{\Gamma}-L_z\bar{C})\end{bmatrix},$$

$$P_x=\mathrm{diag}\{XP_{l,1}^{-1}X^T,\ XP_{l,2}^{-1}X^T,\ XP_{l,3}^{-1}X^T\}.$$

Given that $P_l = \mathrm{diag}\{P_{l,1},\ P_{l,2},\ P_{l,3}\}$ are positive-definite matrices, we can have $P_{l,d} > 0$ $(d = 1, 2, 3)$, which is followed by $P_{l,d}^{-1} > 0$. Then, it can be derived that:

$$(P_{l,d} - X)P_{l,d}^{-1}(P_{l,d} - X)^T = P_{l,d} - X - X^T + XP_{l,d}^{-1}X^T \geq 0,$$

which means that $-XP_{l,d}^{-1}X^T \leq P_{l,d} - X - X^T$.

Moreover, considering that the SVD of the full-rank matrix $\bar{B}$ can be expressed as $\bar{B} = \vartheta \begin{bmatrix} S \\ 0 \end{bmatrix} \nu^T$, where $\vartheta^T\vartheta = I$ and $\nu^T\nu = I$, then according to Lemma 1, for the matrix $X = \vartheta \begin{bmatrix} M & 0 \\ 0 & N \end{bmatrix} \vartheta^T$, it has $X\bar{B} = \bar{B}\tilde{X}$ with $\tilde{X} = XS^{-1}MSX^T$. Finally, by substituting $X\bar{B}$ and $-XP_{l,d}^{-1}X^T$ in Eq. (26) with $\bar{B}\tilde{X}$ and $P_{l,d} - X - X^T$, respectively, and defining $K_z = \tilde{X}^{-1}Y_z$ and $L_z = X^{-1}Z_z$, Eq. (25) can be obtained. Thus, the proof of the theorem is completed. □

Remark 3. In Theorem 2, the approach for designing secure synchronization controllers under the envisioned communication environment is specifically introduced. Although the controller gains are derived using LMIs based on fixed system parameters, the controllers do not need to be structurally redesigned when the parameters change. Thus, the proposed synchronization control method can be applied into diverse practical systems, even those with different system parameters, that can be modeled by the considered CN.

Remark 4. In this study, unlike the works that also investigate synchronization problem for CNs with partial information exchange [14,15], WTOD protocol is adopted to avoid the potential data collision and the impact of FDI attack is seriously handled, so as to provide a more practical synchronization approach. Although some recent researches have explored the use of commutation protocols to schedule data transmission in CNs with limited network bandwidth [40,41], but the primary objective of these studies is to design effective state estimators rather than synchronization controllers. Our previous work proposed a RR-based synchronization method for CNs [39], but compared to the WTOD-driven synchronization strategy presented in this study, it is less suitable for dynamic scenarios due to the static feature of RR protocol. Focusing on CNs subject to FDI attack, secure synchronization issue has been addressed in the literature [27,42], but our work is based on a different CN model that incorporates partial information exchange and WTOD protocol, which enhances system performance under conditions of incomplete information and constrained communication resources.

4. Simulation results

In this section, a numerical example is presented to illustrate the effectiveness of the proposed synchronization method. To be specific, we consider a CN with three nodes (that is, $N = 3$), each of which possesses three-dimensional information channels (i.e., $n = 3$). The outer coupling relationship between the nodes is described by the matrix $W = [w_{ij}]_{N\times N}$, which is set as:

$$W = \begin{bmatrix} -0.9 & 0.5 & 0.4 \\ 0.5 & -0.7 & 0.2 \\ 0.4 & 0.2 & -0.6 \end{bmatrix},$$

the inner coupling matrix is defined as $\Gamma = diag_3\{0.1\}$ with the coupling strength $\rho = 0.1$; the channel matrices are set to be $H_{12} = diag\{1, 0, 1\}$, $H_{13} = diag\{1, 1, 0\}$, $H_{21} = diag\{0, 1, 1\}$, $H_{23} = diag\{1, 0, 0\}$, $H_{31} = diag\{0, 1, 0\}$, $H_{32} = diag\{0, 1, 1\}$.

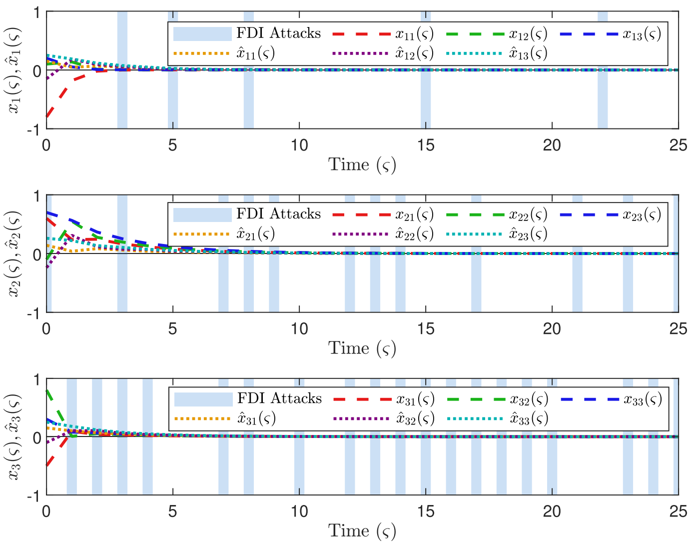

Fig. 2. The observed and real system states under the FDI attack.

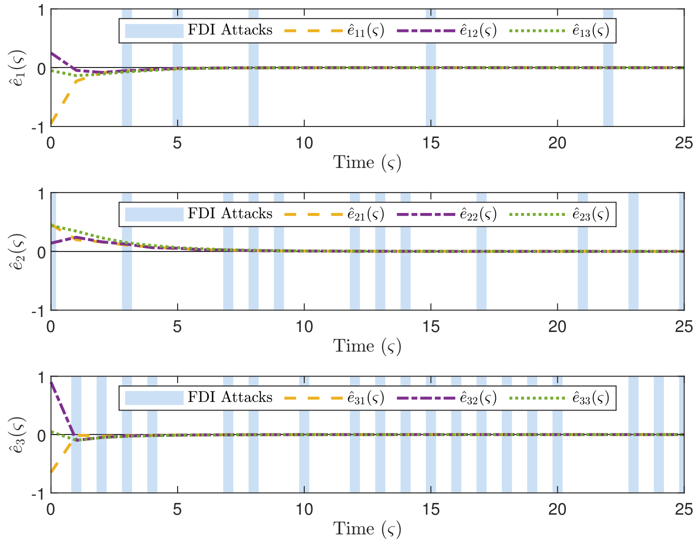

Fig. 3. The estimation errors under the FDI attack.

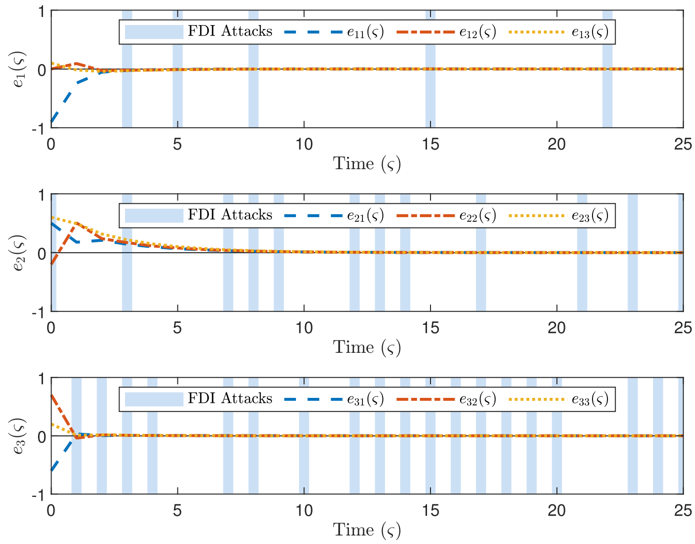

Fig. 4. The synchronization errors under the FDI attack.

The parameter matrices of the system are defined as follows.

$$A = \begin{bmatrix} -0.2 & 0.5 & 0.1 \\ 0.1 & -0.4 & 0.8 \\ 0.1 & -0.1 & 0.7 \end{bmatrix}, B = \begin{bmatrix} -0.1 & 0.1 & 0.2 \\ -0.2 & 0.1 & 0.1 \\ -0.3 & 0 & 0.1 \end{bmatrix}, C = \begin{bmatrix} 0.2 & -0.3 & 0.7 \\ 0.6 & -0.65 & 0.6 \\ 0.5 & 0.7 & -0.6 \end{bmatrix}.$$

The nonlinear function $g(x_i(\varsigma))$ for each node i is set as:

$$g(x_i(\varsigma)) = \begin{bmatrix} 0.1x_{i1}(\varsigma) - 0.3tanh(x_{i1}(\varsigma)) \\ 0.1x_{i2}(\varsigma) - 0.15tanh(x_{i2}(\varsigma)) \\ 0.1x_{i3}(\varsigma) - 0.1tanh(x_{i3}(\varsigma)) \end{bmatrix},$$

where $x_i(\varsigma) = [x_{i1}(\varsigma),\ x_{i2}(\varsigma),\ x_{i3}(\varsigma)]^T$ $(i = 1, 2, 3)$ denotes the state of node i and the upper bound matrix of $g(\cdot)$ is determined as $U = \text{diag}_3\{0.1\}$. Taking into account the influence of the FDI attack, we set $\bar{\alpha}_1 = 0.3$, $\bar{\alpha}_2 = 0.5$, $\bar{\alpha}_3 = 0.7$, and further use $h_i(\varsigma) = 0.1x_i(\varsigma) - \sin(0.1x_i(\varsigma))$ with the upper bound $F = \text{diag}_3\{0.1\}$ to generate the attack signal at each node i. Moreover, the initial states of each system node and the isolated node are set to $x_1(0) = [-0.8,\ 0.1,\ 0.2]^T$, $x_2(0) = [0.6,\ -0.1,\ 0.7]^T$, $x_3(0) = [-0.5,\ 0.8,\ 0.3]^T$, $\hat{x}_1(0) = [0.15,\ -0.15,\ 0.25]^T$, $\hat{x}_2(0) = [0.14,\ -0.24,\ 0.26]^T$, $\hat{x}_3(0) = [0.15,\ -0.1,\ 0.25]^T$, and $s(0) = [0.1,\ 0.1,\ 0.1]^T$.

Based on the simulation parameters mentioned above, the following gain matrices for both observers and controllers can be obtained by solving the LMIs given in Theorem 2.

$$L_{11}=\begin{bmatrix}0.0562 & 0.0453 & 0.1378\\ 0.1288 & 0.0962 & -0.0489\\ 0.1860 & 0.0445 & -0.0521\end{bmatrix},\quad K_{11}=\begin{bmatrix}0.0309 & -0.2306 & 0.1485\\ -0.1369 & 0.6044 & -0.4927\\ 0.0820 & -0.6286 & 0.3947\end{bmatrix},$$

$$L_{12}=\begin{bmatrix}0.0119 & 0.0122 & 0.0867\\ 0.0585 & 0.0974 & -0.0418\\ 0.0986 & 0.0294 & -0.0284\end{bmatrix},\quad K_{12}=\begin{bmatrix}0.0346 & -0.2328 & 0.1535\\ -0.1409 & 0.6344 & -0.5155\\ 0.0893 & -0.6512 & 0.4248\end{bmatrix},$$

$$L_{13}=\begin{bmatrix}0.0172 & -0.0182 & 0.0783\\ 0.0265 & 0.0918 & -0.0466\\ 0.0763 & 0.0096 & -0.0180\end{bmatrix},\quad K_{13}=\begin{bmatrix}0.0341 & -0.2297 & 0.1512\\ -0.1388 & 0.6491 & -0.5214\\ 0.0892 & -0.6586 & 0.4331\end{bmatrix},$$

$$L_{21}=\begin{bmatrix}-0.0098 & 0.0873 & 0.0503\\ 0.0146 & 0.5657 & 0.0266\\ 0.0420 & 0.3168 & -0.0055\end{bmatrix},\quad K_{21}=\begin{bmatrix}0.0813 & -0.3098 & 0.2461\\ -0.2140 & 0.7605 & -0.6566\\ 0.1603 & -0.7696 & 0.5485\end{bmatrix},$$

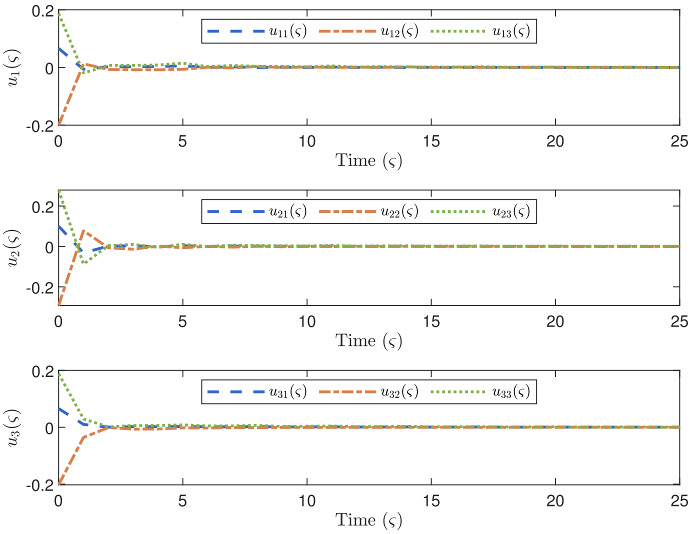

Fig. 5. The trajectories of u_i.

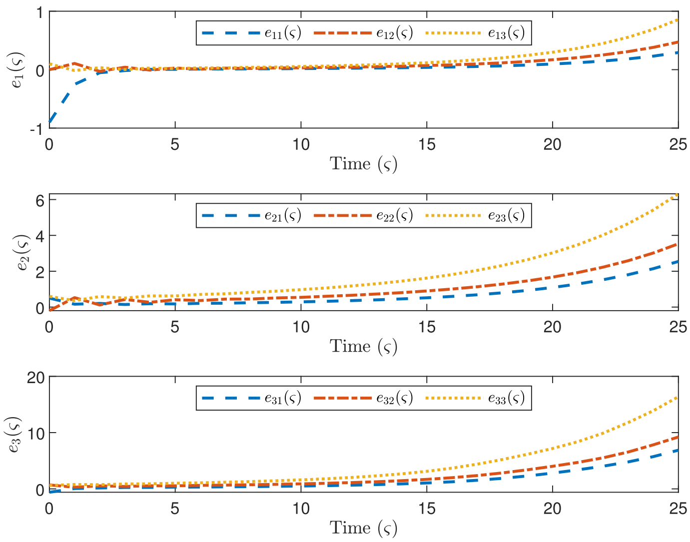

Fig. 6. The synchronization errors without the control inputs.

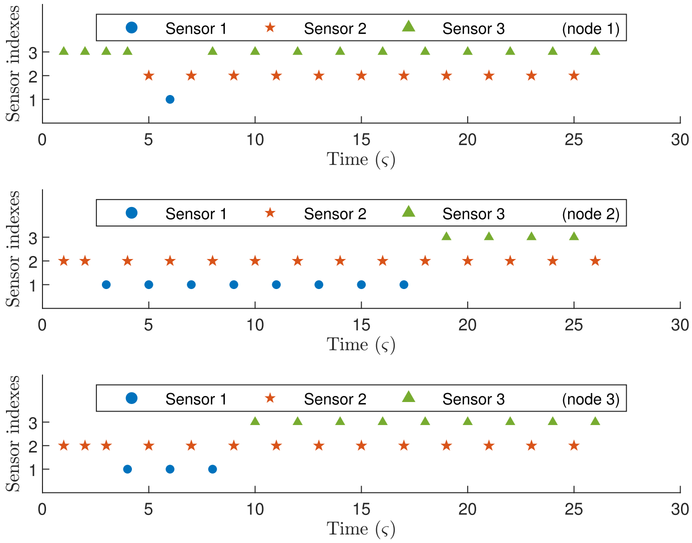

Fig. 7. The working process of WTOD protocol.

$$L_{22}=\begin{bmatrix}0.0050 & -0.0157 & 0.0535\\ 0.0010 & 0.1514 & -0.0381\\ 0.0456 & 0.0492 & -0.0265\end{bmatrix},\quad K_{22}=\begin{bmatrix}0.0353 & -0.2227 & 0.1450\\ -0.1352 & 0.6126 & -0.4919\\ 0.0830 & -0.6220 & 0.4015\end{bmatrix},$$

$$L_{23}=\begin{bmatrix}0.0239 & -0.0381 & 0.0714\\ 0.0049 & 0.1010 & -0.0547\\ 0.0637 & 0.0035 & -0.0217\end{bmatrix},\quad K_{23}=\begin{bmatrix}0.0296 & -0.2171 & 0.1391\\ -0.1285 & 0.6135 & -0.4882\\ 0.0809 & -0.6190 & 0.4047\end{bmatrix},$$

$$L_{31}=\begin{bmatrix}-0.0053 & -0.0150 & 0.0387\\ -0.0065 & 0.1668 & -0.0466\\ 0.0328 & 0.0562 & -0.0420\end{bmatrix},\quad K_{31}=\begin{bmatrix}0.0256 & -0.1888 & 0.1180\\ -0.1116 & 0.5274 & -0.4187\\ 0.0603 & -0.5438 & 0.3240\end{bmatrix},$$

$$L_{32}=\begin{bmatrix}0.0084 & -0.0274 & 0.0526\\ -0.0006 & 0.1091 & -0.0479\\ 0.0452 & 0.0183 & -0.0277\end{bmatrix},\quad K_{32}=\begin{bmatrix}0.0222 & -0.1866 & 0.1135\\ -0.1079 & 0.5225 & -0.4138\\ 0.0610 & -0.5353 & 0.3339\end{bmatrix},$$

$$L_{33}=\begin{bmatrix}0.0245 & -0.0419 & 0.0670\\ 0.0032 & 0.0799 & -0.0569\\ 0.0598 & -0.0098 & -0.0213\end{bmatrix},\quad K_{33}=\begin{bmatrix}0.0208 & -0.1866 & 0.1127\\ -0.1069 & 0.5326 & -0.4189\\ 0.0628 & -0.5400 & 0.3458\end{bmatrix}.$$

The specific simulation results are presented in Figs. 2–7. The system states and their estimations are shown in Fig. 2. It can be found that the observed system states exhibit slight deviations from the real system states even in the presence of the FDI attack. The result is consolidated by Fig. 3 which shows that the estimation errors gradually approach zero, and the effectiveness of the designed observers is thus confirmed. Fig. 4 displays the synchronization errors for all nodes, and it indicates that the errors become negligible with the observer-based control inputs given in Fig. 5. It is also worth noting that without the control inputs, the synchronization errors grow over time as illustrated in Fig. 6. Thus, the effectiveness of the devised controllers in achieving perfect synchronization is fully validated. Moreover, the working process of the employed WTOD protocol is demonstrated in Fig. 7, which reveals that only one sensor is selected for data transmission at each time instant, and thus the data congestion caused by bandwidth constraints can be prevented.

5. Conclusion

In this article, an observer-based synchronization control method has been proposed for a class of CNs subject to partial information exchange, bandwidth constraints, and FDI attack. Specifically, by introducing the channel matrix to depict partial information exchange, the system model that addresses the inherent limitations in data transmission between nodes has been constructed. To mitigate the influence of bandwidth constraints, WTOD protocol has been employed at each node to enable conflict-free and efficient transmission of measurement signals by prioritizing the most important data. Furthermore, the vulnerability of data delivery to FDI attack has been identified, then the secure observer-assisted synchronization controllers have been developed by establishing a synchronization error system and exploring the stability conditions of the system. Eventually, the performance of the presented work has been validated through extensive simulations. It is important to note that the partial information exchange is depicted by 0-1 channel matrices in this study. However, considering the practical realities of communication systems, it is more accurate to employ probabilistic matrices to represent the likelihood of different channel states, which will be investigated in our future work.

Data availability

The data that has been used is confidential.

Acknowledgments

This work is supported in part by the National Natural Science Foundation of China under Grant 62373252 and Grant 62273174, in part by the Natural Science Foundation of Jiangsu Province of China under Grant BK20230063.

References

[1] L. Sedghi, V. DiMassa, A. Harrington, S.V. Lynch, Y.L. Kapila, The oral microbiome: role of key organisms and complex networks in oral health and disease, Periodontology 2000 87 (1) (2021) 107–131.
[2] G. Boeing, OSMnx: New methods for acquiring, constructing, analyzing, and visualizing complex street networks, Comput. Environ. Urban Syst. 65 (2017) 126–139.
[3] C.E. Graafland, J.M. Gutierrez, J.M. Lopez, D. Pazo, M.A. Rodriguez, The probabilistic backbone of data-driven complex networks: an example in climate, Scientific Reports 10 (1) (2020) 11484.
[4] T. Wen, K.H. Cheong, The fractal dimension of complex networks: a review, Inf. Fusion 73 (2021) 87–102.
[5] Y. Chen, Z. Wang, L. Wang, W. Sheng, Mixed H_2/H_∞ state estimation for discrete-time switched complex networks with random coupling strengths through redundant channels, IEEE Trans. Neural Netw. Learn. Syst. 31 (10) (2019) 4130–4142.
[6] Z. Wu, J. Chen, X. Zhang, Z. Xiao, J. Tao, X. Wang, Dynamic event-triggered synchronization of complex networks with switching topologies: asynchronous observer-based case, Appl. Math. Comput. 435 (2022) 127413.
[7] C. Zhou, L. Zemanová, G. Zamora-Lopez, C. Hilgetag, J. Kurths, Structure–function relationship in complex brain networks expressed by hierarchical synchronization, New J. Phys. 9 (6) (2007) 178.
[8] Y. Li, J. Zhang, J. Lu, J. Lou, Finite-time synchronization of complex networks with partial communication channels failure, Inf. Sci. 634 (2023) 539–549.
[9] C. Huang, D.W.C. Ho, J. Lu, J. Kurths, Pinning synchronization in T-S fuzzy complex networks with partial and discrete-time couplings, IEEE Trans. Fuzzy Syst. 23 (4) (2014) 1274–1285.
[10] Q. Cui, L. Li, J. Lu, A. Alofi, Finite-time synchronization of complex dynamical networks under delayed impulsive effects, Appl. Math. Comput. 430 (2022) 127290.
[11] M. Chen, D. Ding, H. Yan, K. Liang, Mode-based triggered protocol for synchronization of switched dynamic networks with semi-Markov kernel and its application, Appl. Math. Comput. 495 (2025) 129336.
[12] X. Hu, L. Wang, C. Zhang, Y. He, Fixed-time synchronization of fuzzy complex dynamical networks with reaction-diffusion terms via intermittent pinning control, IEEE Trans. Fuzzy Syst. 32 (4) (2024) 2307–2317.
[13] C. Huang, D.W.C. Ho, J. Lu, Partial-information-based synchronization analysis for complex dynamical networks, J. Franklin Inst. 352 (9) (2015) 3458–3475.
[14] T. Liang, W. Zhang, J. Dong, D. Yang, Fixed/preassigned-time stochastic synchronization of T-S fuzzy complex networks with partial or complete information communication, ISA Trans. 137 (2023) 339–348.
[15] J. Zhang, J. Lu, J. Qiu, J. Liang, Prescribed-time synchronization of complex networks with switching partial information transmission, IEEE Trans. Circuits Syst. II Express Briefs 71 (5) (2024) 2724–2728.
[16] H. Zhang, Y. Liu, Y. Wang, Observer-based finite-time adaptive fuzzy control for nontriangular nonlinear systems with full-state constraints, IEEE Trans. Cybern. 51 (3) (2020) 1110–1120.
[17] P. Selvaraj, R. Sakthivel, C.K. Ahn, Observer-based synchronization of complex dynamical networks under actuator saturation and probabilistic faults, IEEE Trans. Syst., Man, and Cybern. Syst. 49 (7) (2018) 1516–1526.
[18] D. Liu, D. Ye, Pinning-observer-based secure synchronization control for complex dynamical networks subject to DoS attacks, IEEE Trans. Circuits Syst. I Regul. Pap. 67 (12) (2020) 5394–5404.
[19] Y. Zhao, X. Li, R. Rao, Synchronization of nonidentical complex dynamical networks with unknown disturbances via observer-based sliding mode control, Neurocomputing 454 (2021) 441–447.
[20] Z. Gu, T. Yin, Q. Lu, J.H. Park, Resilient event-triggered formation control and secure estimation of multi-UAV systems, IEEE Trans. Ind. Inf. 21 (6) (2025) 4915–4923.
[21] L. Zha, R. Liao, J. Liu, X. Xie, E. Tian, J. Cao, Outlier-resistant distributed filtering over sensor networks under dynamic event-Triggered schemes and DoS attacks, IEEE Trans. Autom. Sci. Eng. 22 (2025) 1152–1162.
[22] G. Franzè, F. Tedesco, D. Famularo, Resilience against replay attacks: a distributed model predictive control scheme for networked multi-agent systems, IEEE/CAA J. Autom. Sin. 8 (3) (2020) 628–640.
[23] W. Qi, Y. Hou, G. Zong, C.K. Ahn, Finite-time event-triggered control for semi-Markovian switching cyber-physical systems with FDI attacks and applications, IEEE Trans. Circuits Syst. I Regul. Pap. 68 (6) (2021) 2665–2674.
[24] Z. Gu, Y. Fan, F. Yang, E. Tian, Event-triggered T-S fuzzy load frequency control with variable probabilistic release for renewable energy integrated power systems, IEEE Trans. Autom. Sci. Eng. 22 (2025) 8492–8510.
[25] L. Zha, J. Miao, J. Liu, E. Tian, C. Peng, Privacy-preserving distributed estimation over sensor networks with multistrategy injection attacks: a chaotic encryption scheme, IEEE Trans. Syst. Man and Cybern. Syst. 55 (7) (2025) 4969–4978.
[26] R. Pan, Y. Tan, D. Du, S. Fei, Adaptive event-triggered synchronization control for complex networks with quantization and cyber-attacks, Neurocomputing 382 (2020) 249–258.
[27] J. Li, Y. Huang, H. Rao, Y. Xu, R. Lu, Finite-time cluster synchronization for complex dynamical networks under FDI attack: a periodic control approach, Neural Netw. 165 (2023) 228–237.
[28] D. Yue, E. Tian, Q.-L. Han, A delay system method for designing event-triggered controllers of networked control systems, IEEE Trans. Automat. Contr. 58 (2) (2012) 475–481.
[29] X. Zhang, G. Yang, Optimal sensor attacks in cyber-physical systems with Round-Robin protocol, Inf. Sci. 548 (2021) 85–100.
[30] X. Zheng, Y. Kang, H. Li, J. Li, Multiple description encoding-decoding-based resilient filtering for complex networks under the Round-Robin protocol, Appl. Math. Comput. 458 (2023) 128250.
[31] H. Fu, J. Li, F. Han, N. Hou, H. Dong, Outlier-resistant observer-based H_∞ PID control under stochastic communication protocol, Appl. Math. Comput. 411 (2021) 126535.
[32] J. Liu, J. Ke, J. Liu, X. Xie, E. Tian, Secure event-triggered control for IT-2 fuzzy networked systems with stochastic communication protocol and FDI attacks, IEEE Trans. Fuzzy Syst. 32 (3) (2024) 1167–1180.
[33] Y. Shen, Z. Wang, B. Shen, H. Dong, Outlier-resistant recursive filtering for multisensor multirate networked systems under weighted try-once-discard protocol, IEEE Trans. Cybern. 51 (10) (2020) 4897–4908.
[34] J. Liu, E. Gong, L. Zha, E. Tian, X. Xie, Observer-based security fuzzy control for nonlinear networked systems under weighted try-once-discard protocol, IEEE Trans. Fuzzy Syst. 31 (11) (2023) 3853–3865.
[35] J. Liu, L. Zha, W. Jiang, E. Tian, Stabilization of uncertain parabolic PDE systems under weighted try-once-discard protocol with actuator failures, IEEE Trans. Ind. Inf. 21 (7) (2025) 5603–5611.

[36] D. Wang, Z. Wang, B. Shen, Q. Li, H_∞ Finite-horizon filtering for complex networks with state saturations: the weighted try-once-discard protocol, Int. J. Rob. Nonlinear Contr. 29 (7) (2019) 2096–2111.

[37] C. Liu, L. Yang, J. Tao, Y. Xu, T. Huang, Set-membership filtering for complex networks with constraint communication channels, Neural Netw. 152 (2022) 479–486.

[38] Y. Zhang, M. Luo, J. Cheng, I. Katib, K. Shi, Security-protocol-based sliding mode control for singularly perturbed complex networks with dual-layer switching mechanism, Nonlinear Dyn. 112 (3) (2024) 1971–1995.

[39] Y. Li, F. Song, J. Liu, X. Xie, E. Tian, S. Fei, Round Robin-Based synchronization control for discrete-time complex networks with probabilistic coupling delay and deception attacks, IEEE Trans. Syst. Man, Cybern. Syst. 54 (7) (2024) 4425–4436.

[40] X. Wan, Z. Wang, M. Wu, X. Liu, H_∞ State estimation for discrete-time nonlinear singularly perturbed complex networks under the Round-Robin protocol, IEEE Trans. Neural Netw. Learn. Syst. 30 (2) (2019) 415–426.

[41] N. Hou, H. Dong, Z. Wang, H. Liu, A partial-node-based approach to state estimation for complex networks with sensor saturations under random access protocol, IEEE Trans. Neural Netw. Learn. Syst. 32 (11) (2020) 5167–5178.

[42] H. Huang, J. Xu, J. Wang, X. Chen, Reinforcement learning-based secure synchronization for two-time-scale complex dynamical networks with malicious attacks, Appl. Math. Comput. 479 (2024) 128840.